Published in final edited form as:

Conf Proc IEEE Eng Med Biol Soc. 2018 July ; 2018: 3418–3421. doi:10.1109/EMBC.2018.8512967.

Automated Kidney Segmentation for Traumatic Injured Patients through Ensemble Learning and Active Contour Modeling

Negar Farzaneh[1], **S.M. Reza Soroushmehr**[1,2], **Hirenkumar Patel**[3], **Alexander Wood**[1], **Jonathan Gryak**[1], **David Fessell**[4,5], and **Kayvan Najarian**[1,2,5]

[1]Department of Computational Medicine and Bioinformatics, University of Michigan, Ann Arbor, MI, USA

[2]Michigan Center for Integrative Research in Critical Care University of Michigan, Ann Arbor, MI, USA

[3]Department of Emergency Medicine, University of Michigan, Ann Arbor, MI, USA

[4]Department of Radiology, University of Michigan, Ann Arbor, MI, USA

[5]Department of Emergency Medicine, University of Michigan, Ann Arbor, MI, USA

Abstract

Traumatic abdominal injury can lead to multiple complications including laceration of major organs such as kidneys. Contrast-enhanced Computed Tomography (CT) is the primary imaging modality for evaluating kidney injury. However, the traditional visual examination of CT scans is time consuming, non-quantitative, prone to human error, and costly. In this work we propose a kidney segmentation method using machine learning and active contour modeling. We first detect an initialization mask inside the kidney and then evolve its boundary. This model is specifically developed and evaluated on trauma cases. Our experimental results show the average recall score of 92.6% and average Dice similarity value of 88.9%.

Keywords

Kidney segmentation; Abdominal trauma; Active contour modeling; Texture analysis; Machine learning

I. INTRODUCTION

Automated decision support systems could help physicians in clinical diagnosis, prognosis and ultimately treatment planning. As of the main inputs of such systems is images, a major component of these systems is image processing, and in particular image segmentation. Anatomical structures and other regions of interest are delineated using image segmentation techniques. However, due to biological variations, existing noise and artifacts that are inherent components of medical images, grayscale similarity between the border of an organ and neighboring tissue, and different scanner settings, medical segmentation is a challenging task. In the past three decades many segmentation techniques have been proposed for different medical applications such as anatomical structure segmentation [1]–[6] and pathology detection [7]–[10]. The aims of these methods are to improve upon conventional

user-guided segmentation methods and also to delineate images for further quantitative analysis (e.g., volumetric measurement) [1], which provides important information for diagnosis/prognosis . The availability of such information in real-time for trauma injury patients is of utmost importance as time is more crucial to outcome. Therefore, developing fast and accurate computational methods to segment the organs and detect injuries is of great value.

In this paper we focus on trauma injury patients and design an automated method to segment the kidneys from Computed Tomography (CT) scans. Contrast-enhanced CT scans is the modality of choice to detect kidney injuries. Contrast enhancement is the process whereby the optimal visible difference among adjacent structures (e.g., a lesion and the normal surrounding structure) is obtained by injecting a contrast agent. Depending on the timing of the CT scan capture after initiation of contrast agent injection, abdominal CT contrast phase can be divided into different phases such as arterial, portal venous, nephrogenic and delayed [11]. Each contrast phase highlights certain types of tissues or injuries and thus contrast phase knowledge leads to more accurate CT image segmentation and lesion classification [12], [13]. However, this information is often missing or inaccurate [14]. Therefore, it is important for an algorithm to be generalizable over all types to be applicable in real clinical settings.

A number of automated methods have been proposed to segment the kidneys using CT scans. Lin *et al.* [1] categorized kidney segmentation methods to 1) thresholding and region-based; 2) knowledge-based; and 3) deformable methods. They also designed a method using the geometric location of kidney to detect seed points as well as adaptive region growing to segment the kidneys. This method is based upon the assumption that kidney is visible in the middle slice of the set of abdominal CT scan, which might not be always true. Skalski *et al.* presented a kidney segmentation model that falls in the category of deformable models [2]. In this work, ellipsoid shape constraints are incorporated into the level-set formulation. In addition to three kidney segmentation categories introduced in [1], over the last decade a body of literature has focused on machine learning approaches such as deep learning and ensemble learning (such as random forest) methods to address this problem. Khalifa *et al.* [3] , [4] designed a 3-D kidney segmentation algorithm using a random forest classifier and adaptive shape modeling. Wolz *et al.* [5], [6] introduced a hierarchical subject-specific atlas generation model to address high inter-subject variability. This model requires a large training dataset to be practical. Additionally, all of the CT scans were captured at the portal venous contrast phase; therefore, although this model shows promising results its accuracy and generalizability over heterogeneous cohorts in different clinical settings are questionable.

In this paper we propose an automated kidney segmentation method by implementing machine learning and active contour modeling. This algorithm is designed based on CT scans without prior knowledge of contrast phase. Moreover, our focus is on patients admitted to the trauma service which adds to heterogeneity in our medical data.

The remainder of this paper is structured as follows. In section II, we lay out the proposed approach, as well as our previously introduced method for abdominal cavity alignment. We

describe our method in detail in section III and IV. In section V, our dataset is described. In section VI we discuss our experimental results and conclude the paper.

II. Method

The schematic diagram of the proposed method is depicted in Figure 1. In order to detect the kidneys, we first find and align the abdominal cavity. Towards this end, we adjust the image contrast, segment the main bones' mask, and accordingly register each 3-D CT image set using orientation, scaling and transformation functions. For more details of abdominal contour alignment refer to our previous work introduced in [15]. Next, a 3-D initialization mask will be detected within the abdominal cavity. For this purpose, we divide the abdominal cavity to small patches using a superpixel algorithm, and for each patch we extract multiple features. These features will be used in our random forest classifier to detect potential initialization voxels. Finally, an adaptive contour model is designed to evolve the boundary of the mask. This method is performed twice to segment the left and the right kidneys independently, after which the results from each execution are combined to produce the final segmentation.

III. Initialization Mask Detection

We use an efficient segmentation method called "active contour" that starts with an initialization mask and throughout a number of iterations the mask is evolved. In order to accurately segment the kidney using this technique, it is crucial to choose an initial mask accurately. To accomplish this, a machine learning algorithm is used to determine the probability of each pixel belonging to the kidney region. An adaptive thresholding method is then applied on the probability values to determine a 3-D volume as the initial mask.

A. Classification Model

We intend to extract features representing each pixel in an axial plane. However, extracting features for every single pixel is computationally intensive while providing redundant information. Thus, we first group a set of adjacent pixels to build superpixels using the simple linear iterative clustering (SLIC) algorithm [16]. Next, we select a window W of 25 × 25 pixels, around the center of the mass of each superpixel. A set of statistical, textural, and spatial features are extracted from each superpixel using its corresponding W. Statistical information includes minimum, maximum, average, standard deviation skewness, and kurtosis of intensities of pixels within W. Textural features consist of smoothness, entropy, Laplacian of Gaussian, and Gabor filter-based features. Gabor features are calculated in eight evenly spaced orientations and four different frequencies. Laplacian of Gaussian highlights sharp intensity changes and is useful for edge detection. Finally, spatial features are determined as the location of a superpixel in the Cartesian coordinate system.

To determine the probability score of each superpixel belonging to the kidney region, a random forest classifier is trained using patient-wise 10-fold cross-validation. These models are trained once and loaded for each subsequent segmentation run. Conventionally, in machine learning classification models a fixed threshold is applied as a cut-off on the probability score of each sample point to determine its class. However, due to heterogeneous

representations of kidneys in CT scans, mainly due to various contrast phase and inter-patient anatomical variability, we do not apply a fixed threshold to the probability score. Instead, we apply an adaptive threshold model to determine the initial mask.

B. Adaptive Probability Thresholding

In this section, we apply an adaptive threshold on the probability score to segment out a 3-D initialization volume inside the kidney. To calculate this threshold, T, we start with the maximum threshold value of 1 and gradually decrease the threshold value by Δ until we segment out a 3-D connected component larger than a predefined volume V_{min}. Therefore, the optimum cutoff threshold is computed by:

$$T = max\left\{1 - k\Delta \middle| V_{1-k\Delta} > V_{min}, k = 0, 1, \ldots, \left\lfloor \frac{1}{\Delta} \right\rfloor \right\}$$

where V_T is the volume of the current largest connected component by applying cutoff value of T.

IV. Kidney Surface Modeling using Active Contour model

At this stage, the boundary of the initialization mask calculated in the previous section is evolved by using 3- D active contour modeling. Active contour modeling evolves the initialization mask in an iterative process to be entirely constrained by the border of the desired object. As in many CT scans the edges between kidneys and neighboring organs such as liver are smooth, or injuries might blur the boundaries, edge-based active contour models are not effective. Thus, we implement an active contour model known as Chan-Vese that is proposed to segment objects without welldefined edges [17]. The Chan-Vese model is based on a levelset formulation and Mumford-Shah segmentation techniques, and is widely used in medical image processing.

In this work, after each fixed number of iterations (10) , the evolved region is first refined based on intensity and then by its 3-D representation (Figure 2).

To refine the region based on intensity, the mean, μ, and standard deviation, σ, of the corresponding evolved region on the original image are calculated first. Then, voxels with intensity values outside $[\mu - \sigma, \mu + \sigma]$ are excluded. Due to the contrast phase or imaging settings, the pixels' intensity of kidney and liver might be very close to each other and hence part of the liver might be mistakenly segmented as kidney. Thus, approximate mean intensity values of kidneys and liver are used to find CT scans with such characteristics. Mean intensity of kidneys is easily calculated by averaging the voxel intensity of the current mask. In order to estimate the mean intensity of the liver, we use the liver probability atlas proposed in [15]. We select all voxels belonging to the liver with the highest probability and calculate their mean intensity value. For a CT scan with low intensity contrast between liver and kidneys, a stricter condition is applied to exclude all voxels with intensity less than $\mu - 0.5 \times \sigma$ (Figure 3). Next, only voxels belonging to the largest connected component are selected as the kidney has a contiguous representation. Moreover, to prevent over-segmentation and minimize the running time, the volume of the current mask is calculated.

If the volume is larger than a hard threshold, the iterative process will be terminated. This threshold is based on the maximum of kidney volumes.

V. Dataset

In total, 1750 CT images from 35 patients are studied. All CT scans are collected from patients who were admitted to the trauma service at the University of Michigan Health System. Among 35 patients, 22 were transferred to the Intensive Care Unit (ICU), 7 of them to a general admission and non-specialty unit bed, 5 to the operating room and 1 patient died. All images were collected using the GE Medical System scanner and share the same slice thickness of 5 *mm*, however, contrast phases are different and unknown. Figure 4 shows variations caused by contrast phase and trauma.

VI. EXPERIMENTAL RESULT AND CONCLUSION

We compared our segmentation results with the manually annotated ground truth verified by a radiologist. We used 10fold cross-validation to evaluate the random forest initialization mask detection model. Each fold includes CT scans from 3 or 4 patients. Except for the left kidney in one patient our algorithm correctly detected the initialization mask entirely within the kidney region. Our final segmentation results show voxel-wise Dice, recall, precision value of 88.9% , 92.6% , and 86.4% respectively.

Table II shows the comparison between the performance of our model and state-of-the-art methods.

Note that each model is developed on a different dataset with different imaging settings and potentially different populations of interest, thus direct comparison cannot be made from this table. For example, Khalifa *et al.* developed their method on CT images collected from 20 subjects while each subject has high resolution CT scan (slice thickness of 0.9 *mm*) at 3 known contrast phases as pre-, post-, and delayed contrast phases [3], [4].

Moreover, although our results are promising, in one severe case our algorithm was unable to segment cysts - preexisting abnormal fluid-filled sacs that are not considered as trauma; while in ground truth these are considered as parts of the kidneys.

In conclusion, our algorithm unlike the previous methods is developed and evaluated on CT images collected from trauma patients at dissimilar contrast phases. The accuracy of the algorithm can be improved by expanding the dataset in our future work. Moreover, we will incorporate kidney shape priors into the active contour function.

Acknowledgment

This material is based upon work supported by the National Science Foundation under Grant No. 1500124.

Negar Farzaneh is supported by the University of Michigan NIH NIGMS Bioinformatics Training Grant (T 32 GM070499).

References

[1]. Lin Daw-Tung, Lei Chung-Chih, and Hung Siu-Wan. Computer-aided kidney segmentation on abdominal CT images. IEEE transactions on information technology in biomedicine, 10(1):59–65, 2006. [PubMed: 16445250]

[2]. Skalski Andrzej, Heryan Katarzyna, Jakubowski Jacek, and Drewniak Tomasz. Kidney segmentation in CT data using hybrid level-set method with ellipsoidal shape constraints. Metrology and Measurement Systems, 24(1):101–112, 2017.

[3]. Khalifa Fahmi, Soliman Ahmed, Dwyer Amy C, Gimel'farb Georgy, and El-Baz Ayman. A random forest-based framework for 3D kidney segmentation from dynamic contrast-enhanced CT images. In Image Processing (ICIP), 2016 IEEE International Conference on, pages 3399–3403. IEEE, 2016.

[4]. Khalifa Fahmi, Soliman Ahmed, Elmaghraby Adel, Gimelfarb Georgy, and El-Baz Ayman. 3D kidney segmentation from abdominal images using spatial-appearance models. Computational and mathematical methods in medicine, Volume 2017, 2017.

[5]. Wolz Robin, Chu Chengwen, Misawa Kazunari, Mori Kensaku, and Rueckert Daniel. Multi-organ abdominal CT segmentation using hierarchically weighted subject-specific atlases. Medical Image Computing and Computer-Assisted Intervention–MICCAI 2012, pages 10 – 17, 2012.

[6]. Wolz Robin, Chu Chengwen, Misawa Kazunari, Fujiwara Michitaka, Mori Kensaku, and Rueckert Daniel. Automated abdominal multiorgan segmentation with subject-specific atlas generation. IEEE transactions on medical imaging, 32(9):1723–1730, 2013. [PubMed: 23744670]

[7]. Liu Jianfei, Wang Shijun, Linguraru Marius George, Yao Jianhua, and Summers Ronald M. Computer-aided detection of exophytic renal lesions on non-contrast CT images. Medical image analysis, 19(1):15 – 29, 2015. [PubMed: 25189363]

[8]. Soler Luc, Delingette Hervé, Malandain Gregoiré, Montagnat Johan, Ayache Nicholas, Koehl Christophe, Dourthe Olivier, Malassagne Benoit, Smith Michelle, Mutter Didier, et al. Fully automatic anatomical, pathological, and functional segmentation from CT scans for hepatic surgery. Computer Aided Surgery, 6(3):131–142, 2001. [PubMed: 11747131]

[9]. Park SJ, Han JK, Kim TK, and Choi BI. Three-dimensional spiral CT cholangiography with minimum intensity projection in patients with suspected obstructive biliary disease: comparison with percutaneous transhepatic cholangiography. Abdominal imaging, 26(3):281–286 , 2001. [PubMed: 11429953]

[10]. Vorontsov Eugene, Chartrand Gabriel, Tang An, Pal Chris, and Kadoury Samuel. Liver lesion segmentation informed by joint liver segmentation. arXiv preprint arXiv:170707734, 2017.

[11]. Birnbaum Bernard A, Jacobs Jill E, and Ramchandani Parvati Multiphasic renal ct: comparison of renal mass enhancement during the corticomedullary and nephrographic phases. Radiology, 200(3):753 – 758, 1996. [PubMed: 8756927]

[12]. Kawashima Akira, Sandler Carl M, Corl Frank M, Clark West O, Tamm Eric P, Fishman Elliot K, and Goldman Stanford M. Imaging of renal trauma: a comprehensive review. Radiographics, 21(3):557 – 574, 2001. [PubMed: 11353106]

[13]. Dayal Madhukar, Gamanagatti Shivanand, and Kumar Atin. Imaging in renal trauma. World journal of radiology, 5(8):275, 2013. [PubMed: 24003353]

[14]. Sofka Michal, Wu Dijia, Suhling Michael, Liu David, Tietjen Christian, Soza Grzegorz, and Kevin Zhou S. Automatic contrast phase estimation in CT volumes. In International Conference on Medical Image Computing and Computer-Assisted Intervention, pages 166 – 174. Springer, 2011.

[15]. Farzaneh Negar, Habbo-Gavin Samuel, Soroushmehr SM Reza, Patel Hirenkumar, Fessell David P, Ward Kevin R, and Najarian Kayvan. Atlas based 3D liver segmentation using adaptive thresholding and superpixel approaches. In Acoustics, Speech and Signal Processing (ICASSP), 2017 IEEE International Conference on, pages 1093–1097. IEEE, 2017.

[16]. Achanta Radhakrishna, Shaji Appu, Smith Kevin, Lucchi Aurelien, Fua Pascal, and Susstrunk Sabine. SLIC superpixels compared to stateof-the-art superpixel methods. IEEE transactions on pattern analysis and machine intelligence, 34(11):2274–2282, 2012. [PubMed: 22641706]

[17]. Chan Tony F and Vese Luminita A Active contours without edges. IEEE Transactions on image processing, 10(2):266–277, 2001. [PubMed: 18249617]

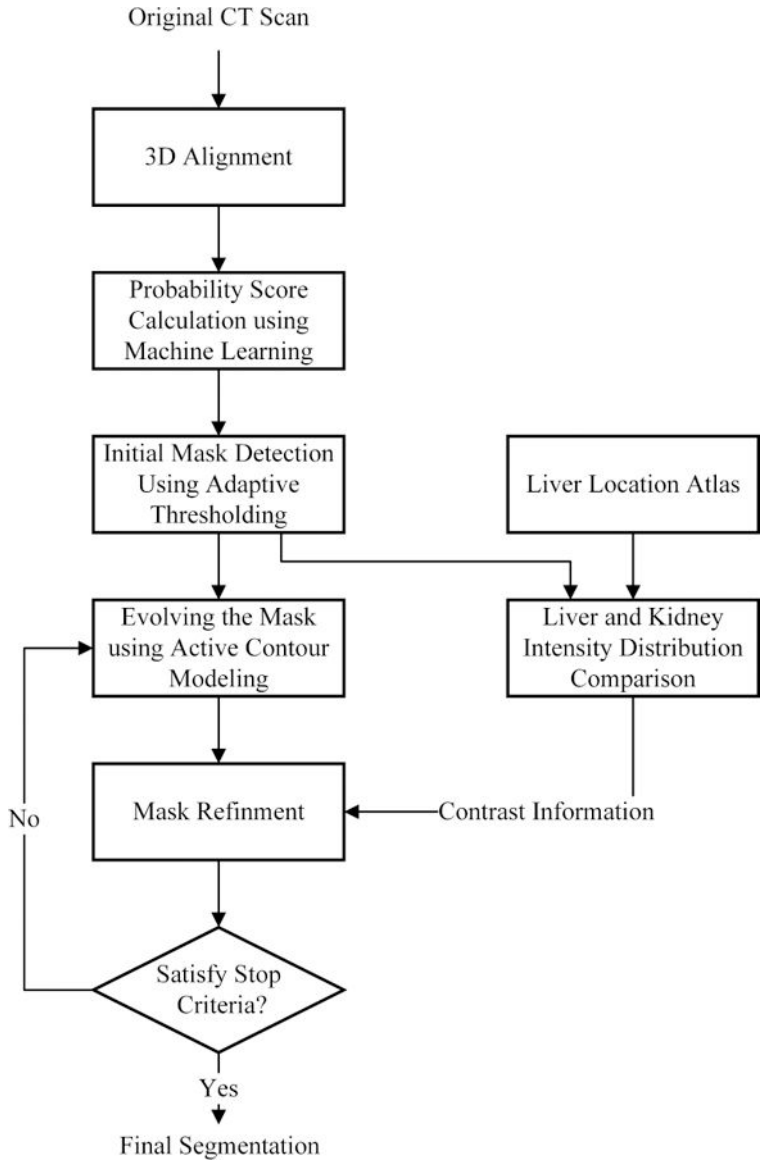

Fig. 1.
Schematic diagram of the proposed kidney segmentation method.

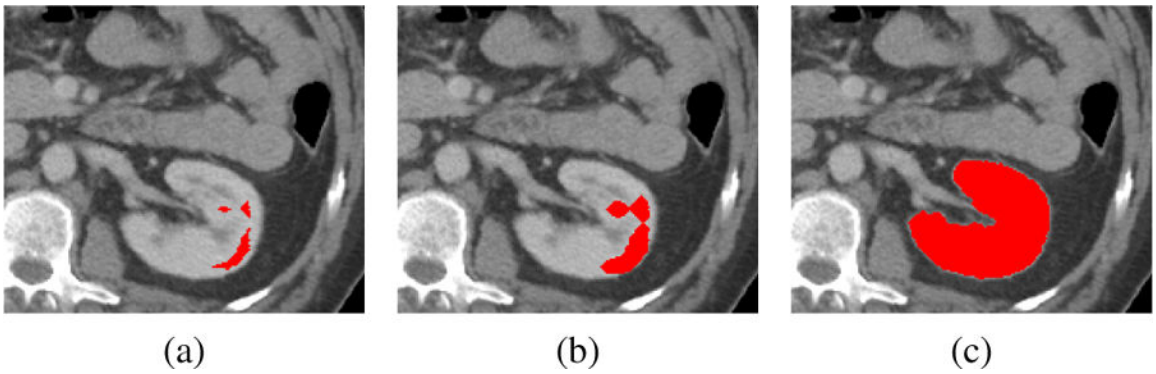

Fig. 2.

(a) The initialization mask is superimposed as the mark on the original image. Note that this image shows a cross section of a 3-D entity, thus the mask may be disconnected in 2-D while it is connected in 3-D. (b) The result of mask evolution after 4 iterations. (c) Final segmentation.

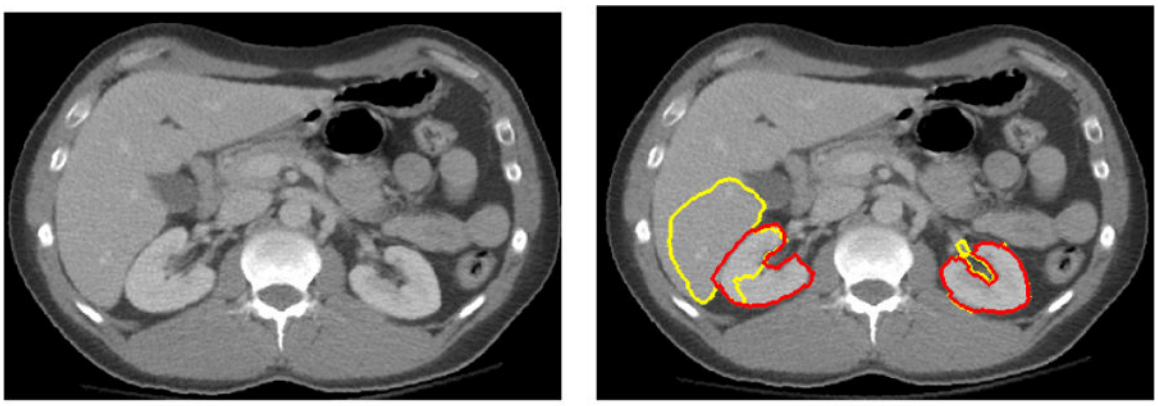

Fig. 3.

(a) The original CT image exhibits low contrast between the kidneys and the liver. (b) The yellow contours show the result without considering the relative intensity distribution of liver and kidney in which the segmentation evolves into the liver. The red contours are the result after incorporating liver probability atlas information. The red contours overlay the yellow ones.

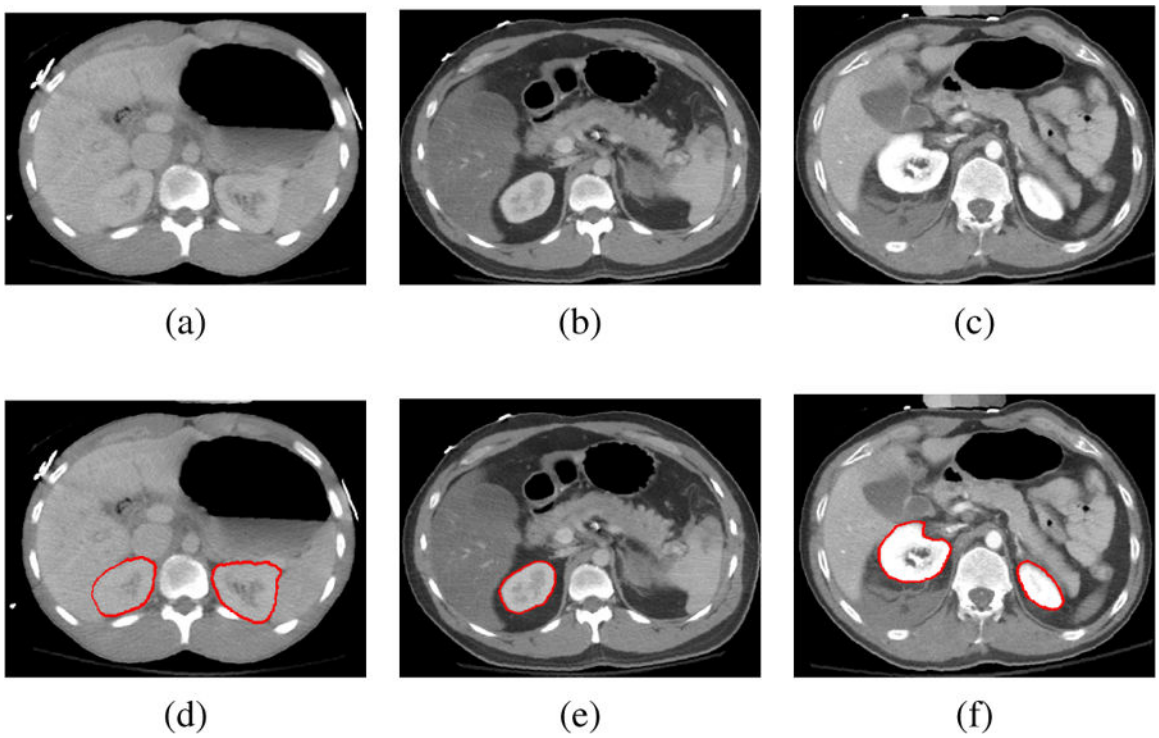

Fig. 4.

(a) A CT image with low contrast between adjacent kidney and liver. (b) Different contrast phases. (c) An injured case with irregularly bright kidney. (d)-(e) The red marks represent the ground truth kidneys contours.

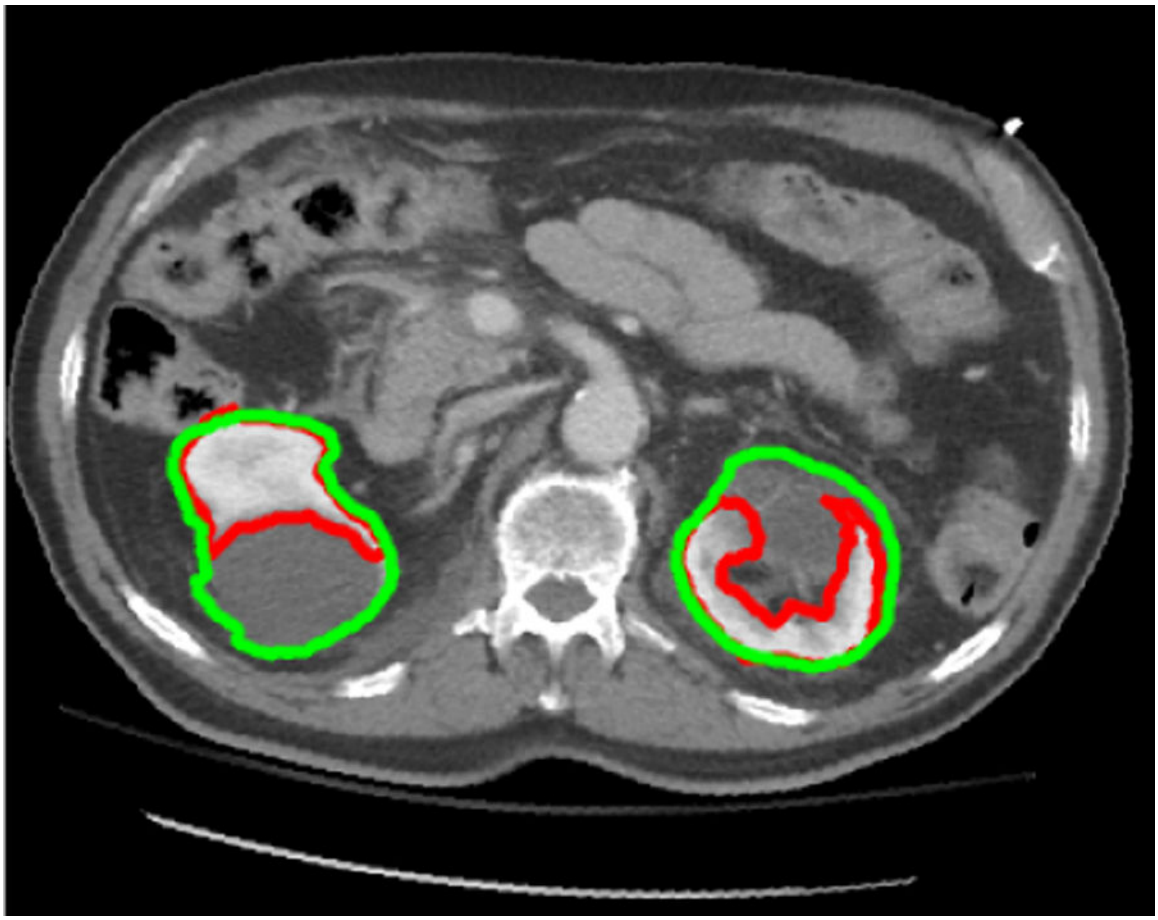

Fig. 5.
The green contours represent the ground truth (including cysts). The red contours are the algorithm final result. The ground truth overlays some parts of segmented result.

TABLE I:

Result of the proposed method.

Segmentation Result	Dice	Recall	Precision
Left kidney	88.6%	90.8%	87.2%
Right kidney	89.0%	94.5%	85.6%

TABLE II:

Comparison of our proposed approach with other existing models.

Methods	Dice(%)
Our proposed method	89%
Lin *et al.* [1]	88.0%
Khalifa *et al.* [3], [4]	97.3 %
Skalski *et al.* [2]	86.2 %